Lateral Force Distributions in Braced-Moment Frames

RALPH M. RICHARD, ERIC KELDRAUK, and JAY ALLEN

ABSTRACT

Braced frames intended to resist wind and seismic loads traditionally have been analyzed and designed as trusses with all joints modeled as pins, such that only the braces provide lateral force resistance. However, frames with gusset plate connections create a rigid joint zone between frame beams and columns, effectively resulting in moment frame behavior, particularly at larger drift angles when braces have yielded or buckled. Described herein are the force distributions for buckling-restrained braced frames (BRBF) subjected to story drift angles, where the lateral resistance of the frame comprises both brace and moment frame action.

Keywords: force distribution, buckling restrained braced frames (BRBF), braced-moment frame.

INTRODUCTION

Braced frames are typically modeled and designed as pinned connected truss members, wherein all lateral resistance is provided by the braces. The design of the gusset plates is subsequently based upon only the transfer of the brace forces to the pin connected beams and columns [*Vertical Bracing Connections—Analysis and Design*, Design Guide 29 (Muir and Thornton, 2014)]. This design rationale has proven acceptable for buckling-restrained braced frames (BRBF) story drift angles at and below that which induces yielding in the braces. However, at story drift angles of approximately 0.0025 (1/400) rad, the braces yield, as shown in the single-story frame pushover analysis in Figure 1, and additional lateral displacement is resisted by moment frame action (Walters et al., 2002). Designers of braced frames often ignore the moment frame action or mitigate it by introducing simple or semi-rigid connections in the braced frame [AISC *Seismic Provisions* Commentary Section F2.6b (2022a)]. Described herein is a rationale that evaluates the moment frame action of the braced frame to lateral loads after the braces yield.

Ralph M. Richard, Professor Emeritus, University of Arizona, Tucson, Ariz. Email: ralph@u.arizona.edu (corresponding)

Eric Keldrauk, Structural Engineer Analyst, Schuff Company, Phoenix, Ariz. Email: eric.keldrauk@gmail.com

Jay Allen, Executive Vice President of Engineering, Schuff Company, Phoenix, Ariz. Email: jayallense@yahoo.com

Paper No. 2022-12R

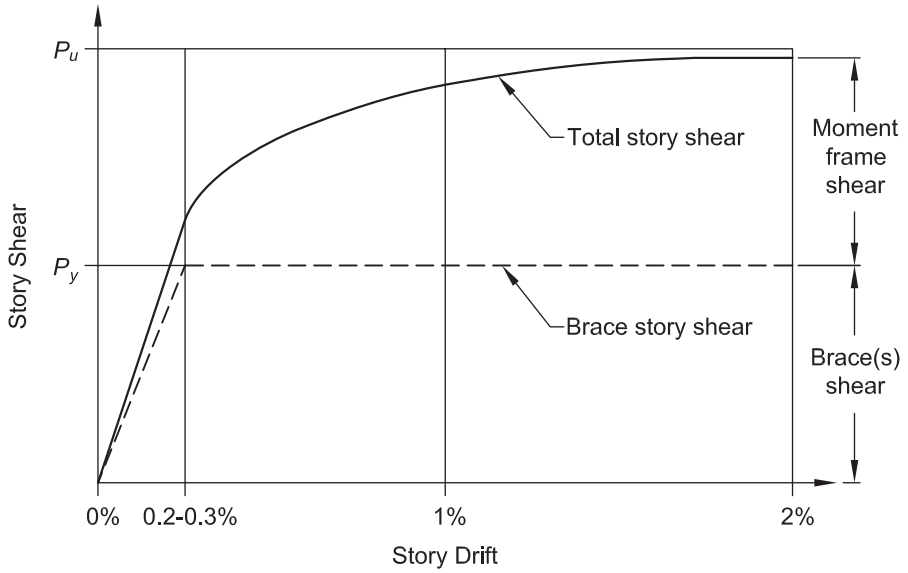

Fig. 1. Typical story shear distribution in a braced frame pushover analysis.

Shown in Figure 2 is a braced frame with typical force distributions using the equivalent lateral force method given in ASCE/SEI 7, *Minimum Design Loads and Associated Criteria for Buildings and Other Structures* (2022). At approximately 0.0025 (1/400) rad, the frame behavior transitions from an idealized braced frame to a combined braced-moment frame, schematically shown in Figure 3, with moment frame resistance resulting from the rigidity of gussets at the beam-column connections. The gusset plates serve a dual purpose of providing a rigid connection joint in addition to transferring the brace force to the beams and columns (Mahin and Patxi, 2002).

Braced-Moment Frame Design Rationale 1: Beam Hinge Mechanism

Figure 4(a) shows a braced-moment frame modeled for analysis of the seismic force distribution as a combination of the force distributions in a braced frame (b) and a moment frame (c). The force distributions in the frames shown in (b) and (c) are based on a seismic drift displacement that results in yielding of the braces in frame (b) and inelastic action in the top and bottom beams in frame (c) based on strong column-weak beam frame design. The forces in frame (b) are based on a pinned truss model with the braces at their yield.

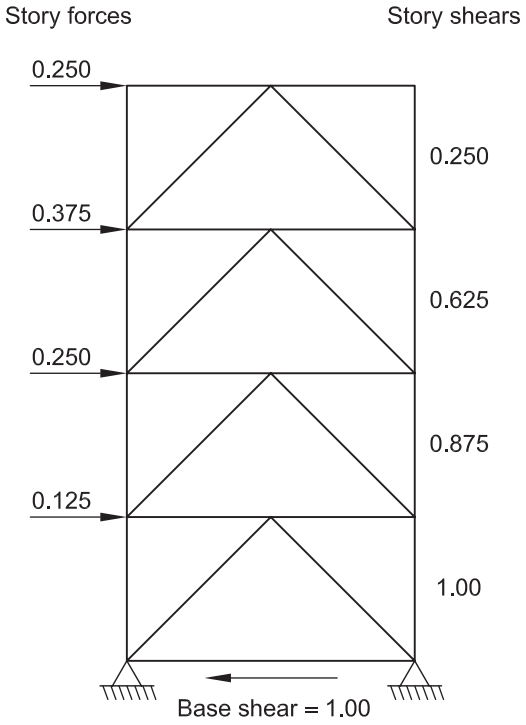

Fig. 2. Typical seismic force distribution in a braced frame using the equivalent lateral force procedure.

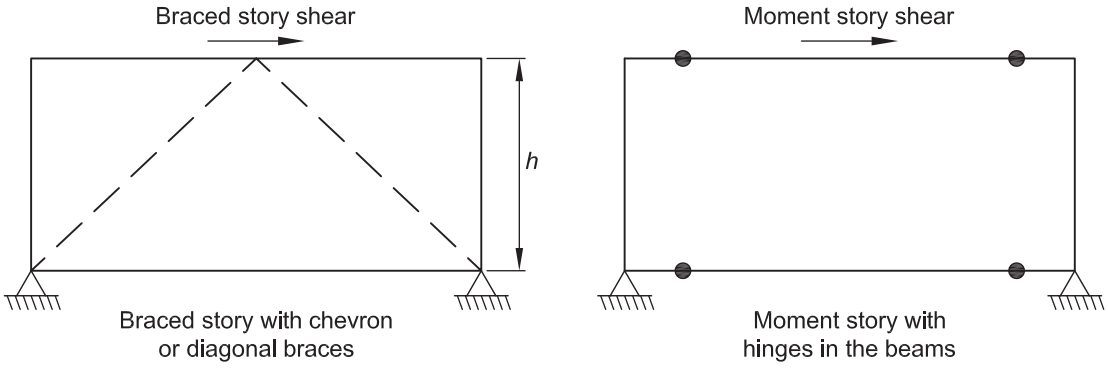

Fig. 3. Idealized single-story braced and moment frames for combined frame model.

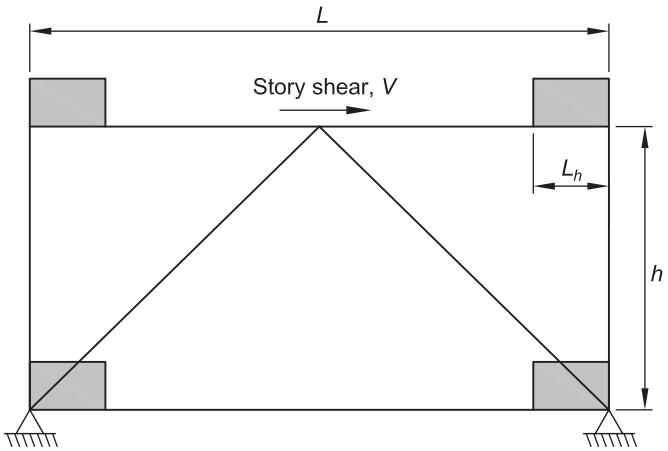

(a) Braced-moment frame

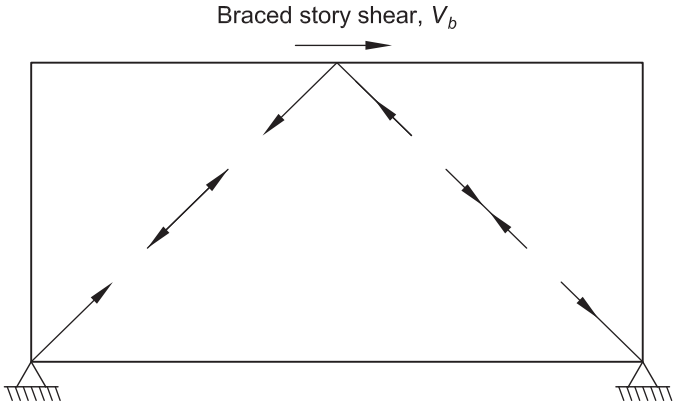

(b) Braced frame

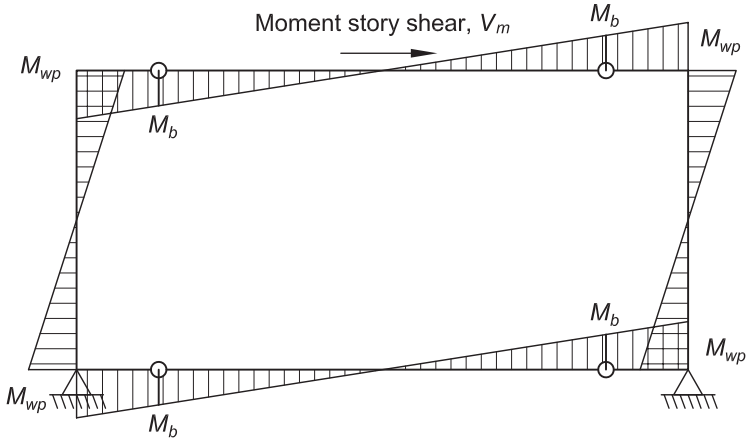

(c) Moment frame force distributions

Fig. 4. Braced-moment frame modeled for analysis of the seismic force distribution as a combination of the force distributions in a braced frame and a moment frame.

The inelastic action in frame (c) is modeled as a four-hinged frame with the hinges located in the beams at the ends of the gusset plates as shown. For a story drift of Δ, the story moment frame shear, V_m may be determined using the virtual work equation by equating external virtual work to internal work:

$$V_m\Delta = 4M_b\theta_{hinge} \tag{1}$$

where M_b is the beam hinge plastic moment, and θ_{hinge} is the hinge rotation.

The plastic hinge rotation in terms of the story drift angle, θ, is:

$$\theta_{hinge} = \theta k_1 = \frac{\Delta k_1}{h} \tag{2}$$

where the constant k_1 is defined in Appendix A and h is the story height.

The beam hinge plastic moment, M_b, is determined as follows:

$$M_b = M_u k_2 \tag{3}$$

where k_2 is a material term that adjusts the pure bending plastic hinge moment, M_u, to account for axial-moment interaction. The derivations of k_1 and k_2 are presented in the appendix of this paper.

Combining the previous equations gives the story shear for the moment story frame (c).

$$V_m = \frac{4M_u k_1 k_2}{h} \tag{4}$$

Referencing Figure 4 and knowing the moment frame story shear, V_m, the brace frame story shear, V_b, is determined as:

$$V_b = V - V_m \tag{5}$$

where V is the frame story shear. The design of the braces is based upon their expected yield stress. This rationale provides the forces in the braces, beams, and columns to design the gusset plates based on a braced-moment frame force distribution.

Braced-Moment Frame Design Rationale 2: Column Hinge Mechanism

Figure 5(a) shows a braced-moment frame modeled for analysis of the seismic force distribution as a combination of the force distributions in a braced frame (b) and a moment frame (c). The force distributions in frames (b) and (c) are based on a seismic drift displacement that results in yielding of the braces in frame (b) and inelastic action in the columns and top beam in frame (c).

The inelastic action in frame (c) is modeled as a four-hinged frame with two hinges located in the column at the end of the bottom gusset plates and two hinges located in the top beam at the ends of the gusset plates as shown. For a story drift of Δ, the story moment frame shear, V_m, may be determined using the virtual work equation by equating external virtual work to internal work:

$$V_m\Delta = 2M_b\theta_{h,b} + 2M_c\theta_{h,c} \tag{6}$$

where M_b is the beam hinge plastic moment, and θ_h is the hinge rotation.

The plastic hinge rotations, $\theta_{h,b}$ and $\theta_{h,c}$, in terms of the story drift angle, θ, are:

$$\theta_{h,b} = \theta k_{1,b} = \frac{\Delta k_{1,b}}{h} \tag{7}$$

$$\theta_{h,c} = \theta k_{1,c} = \frac{\Delta k_{1,c}}{h} \tag{8}$$

where the constants $k_{1,b}$ and $k_{1,c}$ are member specific (see Appendix A for derivation) and h is the story height.

The beam hinge plastic moment, M_b, and column hinge plastic moment, M_c, are determined as follows:

$$M_b = M_{u,b}k_{2,b} \tag{9}$$

$$M_c = M_{u,c}k_{2,c} \tag{10}$$

where $k_{2,b}$ and $k_{2,c}$ are member-specific material terms that adjust the pure bending plastic hinge moments, $M_{u,b}$ and $M_{u,c}$, to account for axial-moment interaction. The derivations of k_1 and k_2 are given in Appendix A.

Combining equations gives the story shear for the moment frame (c).

$$V_m = \frac{2}{h}\left(M_{u,b}k_{1,b}k_{2,b} + M_{u,c}k_{1,c}k_{2,c}\right) \tag{11}$$

Referencing Figure 5 and knowing the moment frame story shear, V_m, the brace frame story shear, V_b, is determined using Equation 5:

$$V_b = V - V_m \tag{5}$$

where V is the frame story shear. The design of the braces is based upon their expected yield stress. This rationale provides the forces in the braces, beams, and columns that are then used to design the gusset plates based on a braced-moment frame force distribution.

Comparison of the Beam-Moment Frame Analysis with Finite Element Analysis

Figure 6 shows the single-story frame used for comparative results. The beams are W21×101, the columns are W14×176, the braces are buckling-restrained braces (BRBs) with a core area of 6 in.^{2}, and the gusset plates are 18 in. × 18 in. Frame members and plates are ASTM A992/A992M (ASTM, 2020) material with F_y = 54 ksi and

ν = 0.30 (Poisson's ratio). The ANSYS finite element analysis (FEA) model is shown in Appendix B. The program used the von Mises yield criterion and kinematic strain hardening with the plastic modulus equal to 2% of the elastic modulus of 29,000 ksi.

A 3.00 in. lateral displacement was applied to the top beam for a 0.025 rad drift angle. Full plastic beam hinges occurred with the hinging region at the ends of the gusset plates. The moment frame action determined by FEA resisted 48% of the frame lateral force at the 0.025 rad drift angle.

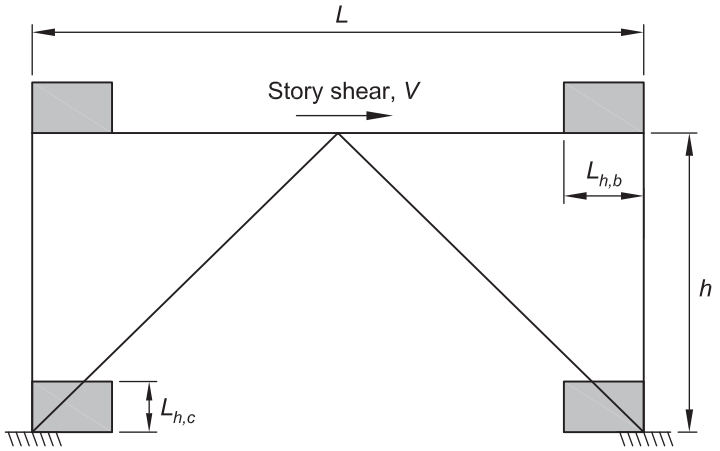

(a) Braced-moment frame

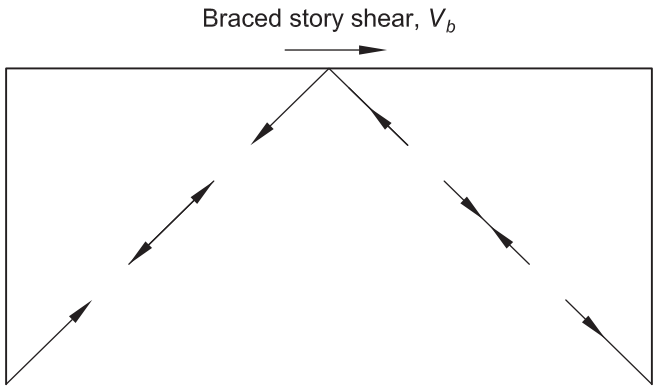

(b) Braced frame

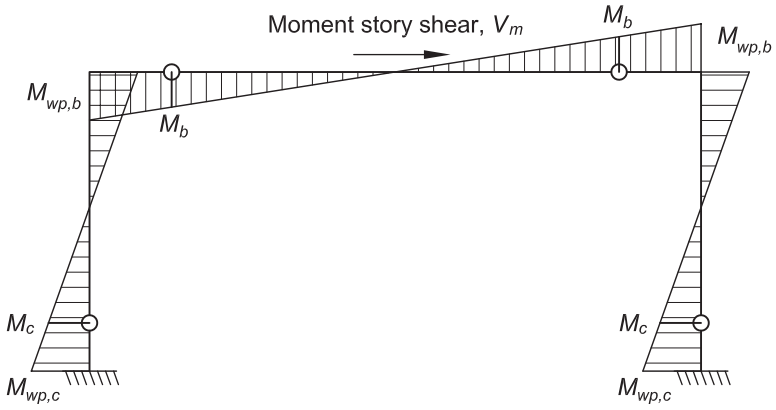

(c) Moment frame force distributions

Fig. 5. Braced-moment frame modeled for analysis of the seismic force distribution as a combination of the force distributions in a braced frame and a moment frame.

For comparative purposes of the beam-moment frame rationale with the FEA results, a lateral force of 1,200 kips was applied at the midpoint of the top beam of the frame shown in Figure 6. The properties of this frame are as follows:

From AISC *Steel Construction Manual* Tables 1-1 and 2-4 (AISC, 2023), the geometric and material properties of the beam and column are as follows:

Beam
W21×101
$A_b = 29.8 \text{ in.}^2$
$Z_{x,b} = 253 \text{ in.}^3$
$d_b = 21.4 \text{ in.}$
$F_y = 54 \text{ ksi (expected)}$

Column
W14×176
$A_c = 51.8 \text{ in.}^2$
$Z_{x,c} = 320 \text{ in.}^3$
$d_c = 15.2 \text{ in.}$
$F_y = 54 \text{ ksi (expected)}$

Frame and gusset geometry:
$L = 240 \text{ in. (working point length of the beam)}$
$h = 120 \text{ in. (working point story height of columns)}$
$L_{p,b} = L_{p,c} = 18 \text{ in. (gusset length/height)}$

The beam axial yield load and pure bending plastic moment are calculated as:

$$P_{y,b} = F_y A_b = (54 \text{ ksi})(29.8 \text{ in.}^2) = 1{,}610 \text{ kips}$$

$$M_{u,b} = F_y Z_{x,b} = (54 \text{ ksi})(253 \text{ in.}^3) = 13{,}700 \text{ kip-in.}$$

The beam hinge length is calculated as the sum of the gusset length and the column halfwidth (i.e., the location of the working point):

$$L_{h,b} = L_p + \frac{d_c}{2} = 18.0 \text{ in.} + \frac{15.2 \text{ in.}}{2} = 25.6 \text{ in.}$$

The beam hinge rotation adjustment factor, $k_{1,b}$, is calculated as:

$$k_{1,b} = 1 + \frac{2L_{h,b}}{L - 2L_{h,b}} \quad \text{(from Eq. A-4)}$$
$$= 1 + \frac{2(25.6 \text{ in.})}{240 \text{ in.} - 2(25.6 \text{ in.})}$$
$$= 1.27$$

The axial load in the beam, P_b, is half the story shear because the columns share the story shear equally. Consequently, k_2 is calculated as:

$$P_b = \frac{V}{2} = \frac{1{,}200 \text{ kips}}{2} = 600 \text{ kips}$$

$$\frac{P_b}{P_{y,b}} = \frac{600 \text{ kips}}{1{,}610 \text{ kips}} = 0.373 > 0.2$$

$$k_{2,b} = \frac{9}{8}\left(1 - \frac{P_b}{P_{y,b}}\right) \quad \text{(from Eq. A-6)}$$
$$= \frac{9}{8}(1 - 0.373)$$
$$= 0.705$$

Using a strain hardening factor of 1.1, the moment capacity of the beam hinge is calculated as:

$$M_b = 1.1 M_u k_{2,b} = 1.1(13{,}700 \text{ kip-in.})(0.705) = 10{,}600 \text{ kip-in.}$$

The moment frame story shear is calculated as:

$$V_m = \frac{4M_b k_{1,b}}{h} = \frac{4(10{,}600 \text{ kip-in.})(1.27)}{120 \text{ in.}} = 449 \text{ kips}$$

This is 37% of the total frame shear of 1,200 kips, which is in agreement with the 48% moment frame action determined by FEA.

The braced frame story shear is calculated as:

$$V_b = V - V_m = 1{,}200 \text{ kips} - 449 \text{ kips} = 751 \text{ kips} \quad (5)$$

This is 63% of the total frame shear of 1,200 kips, which is in agreement with the FEA 52%.

Evaluation of a Lopez Test Frame Using the Column Hinge Mechanism

Shown in Figure 7 are the laboratory test frames designed to evaluate BRBs in braced frames (Lopez et al., 2002, 2004). An analysis for force distributions in the chevron frame is made here.

The properties of the beam and column are as follows:

Beam
W21×93
A_b = 27.3 in.^{2}
$Z_{x,b}$ = 221 in.^{3}
d_b = 21.6 in.
F_y = 54 ksi (expected)

Column
W14×176
A_c = 51.8 in.^{2}
$Z_{x,c}$ = 320 in.^{3}
d_c = 15.2 in.
F_y = 54 ksi (expected)

Frame and gusset geometry:
L = 240 in. (working point length of the beam)
h = 132 in. (working point story height of columns)
$L_{p,b} = L_{p,c}$ = 24 in. (gusset length/height)

The beam axial yield load and pure bending plastic moment are calculated as:

$$P_{y,b} = F_y A_b$$
$$= (54 \text{ ksi})(27.3 \text{ in.}^2)$$
$$= 1{,}470 \text{ kips}$$

$$M_{u,b} = F_y Z_{x,b}$$
$$= (54 \text{ ksi})(221 \text{ in.}^3)$$
$$= 11{,}900 \text{ kip-in.}$$

The beam hinge length is calculated as the sum of the gusset length and the column half width (i.e., the location of the working point):

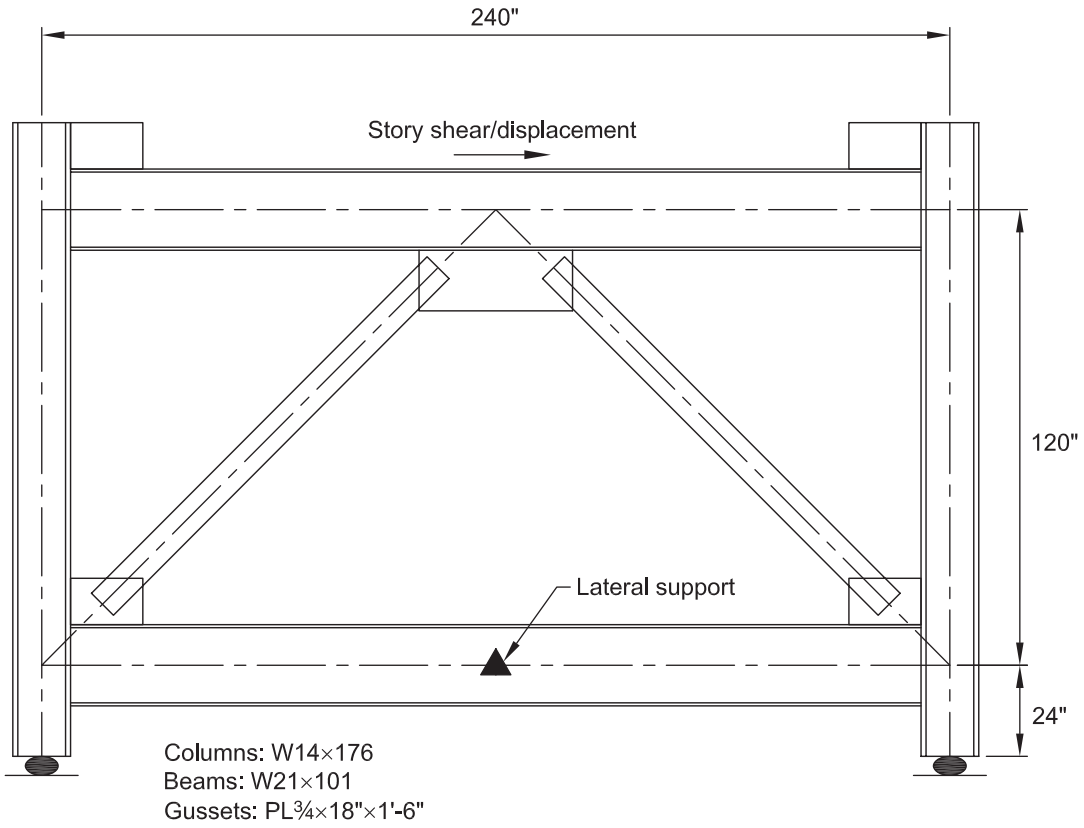

Fig. 6. Single-story chevron test frame.

$$L_{h,b} = L_p + \frac{d_c}{2}$$
$$= 24.0 \text{ in.} + \frac{15.2 \text{ in.}}{2}$$
$$= 31.6 \text{ in.}$$

The beam hinge rotation adjustment factor, $k_{1,b}$, is calculated as:

$$k_{1,b} = 1 + \frac{2L_{h,b}}{L - 2L_{h,b}} \quad \text{(from Eq. A-4)}$$
$$= 1 + \frac{2(31.6 \text{ in.})}{240 \text{ in.} - 2(31.6 \text{ in.})}$$
$$= 1.36$$

The axial load in the beam, P_b, is half the story shear because the columns share the story shear equally. Consequently, k_2 is calculated as:

$$P_b = \frac{V}{2}$$
$$= \frac{1{,}200 \text{ kips}}{2}$$
$$= 600 \text{ kips}$$

$$\frac{P_b}{P_{y,b}} = \frac{600 \text{ kips}}{1{,}470 \text{ kips}}$$
$$= 0.408 > 0.2$$

$$k_{2,b} = \frac{9}{8}\left(1 - \frac{P_b}{P_{y,b}}\right) \quad \text{(from Eq. A-6)}$$
$$= \frac{9}{8}(1 - 0.408)$$
$$= 0.666$$

The column axial yield load and pure bending plastic moment are calculated as:

$$P_{y,c} = F_y A_c$$
$$= (54 \text{ ksi})(51.8 \text{ in.}^2)$$
$$= 2{,}800 \text{ kips}$$

$$M_{u,c} = F_y Z_{x,c}$$
$$= (54 \text{ ksi})(320 \text{ in.}^3)$$
$$= 17{,}300 \text{ kip-in.}$$

The column hinge length is calculated as the gusset height because the working point is at the bottom of the column:

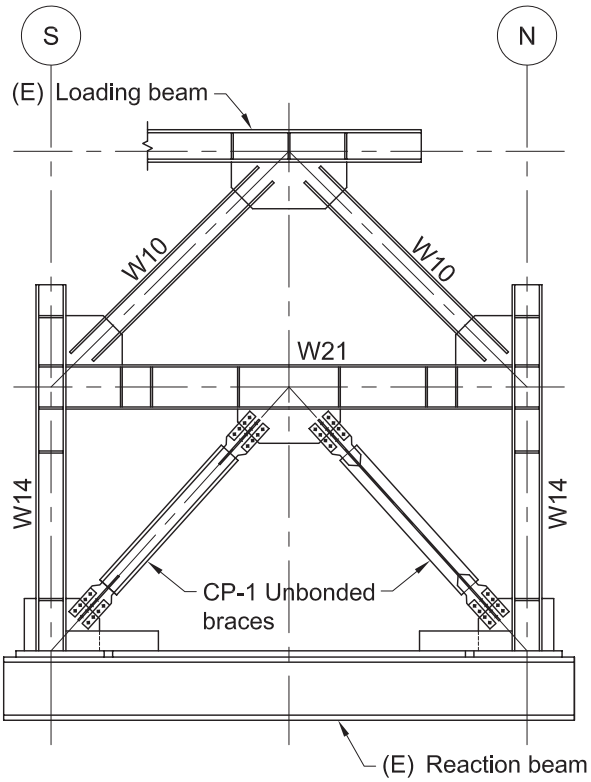

Partial elevation. Setup for test 1.

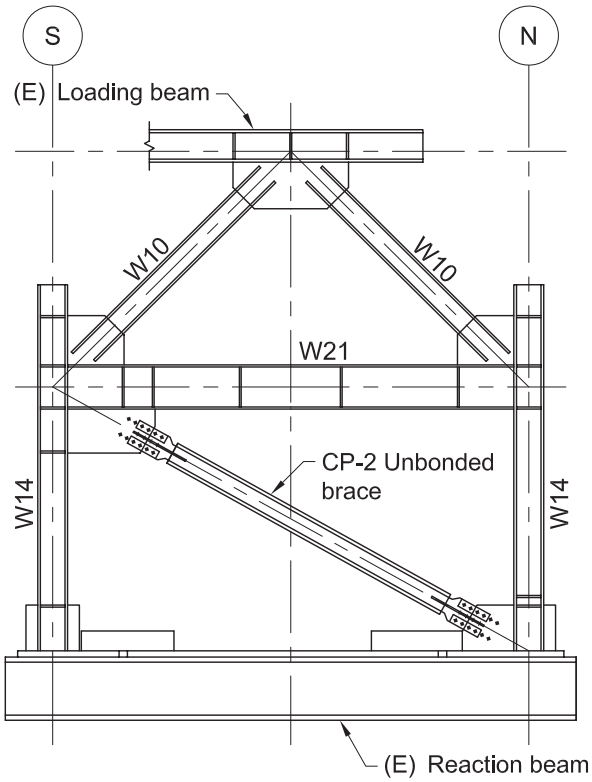

Partial elevation. Setup for tests 2 & 3.

Fig. 7. Laboratory test frames (Lopez et al., 2002, 2004).

$$L_{h,c} = L_{p,c} = 24.0 \text{ in.}$$

The column hinge rotation adjustment factor, $k_{1,c}$, is calculated as:

$$k_{1,c} = 1 + \frac{L_{h,c}}{h - L_{h,c}}$$
$$= 1 + \frac{24.0 \text{ in.}}{132 \text{ in.} - 24.0 \text{ in.}}$$
$$= 1.22$$

The axial load in the column, P_c, is evaluated by equating the frame moment of the axial force to the moment of the shear force [refer to Figure 3 of Lopez et al. (2002), for the frame dimensions]:

$$P_c(240 \text{ in.}) = (1{,}200 \text{ kips})(244 \text{ in.})$$
$$P_c = 1{,}220 \text{ kips}$$

Subsequently, $k_{2,c}$ is calculated as:

$$\frac{P_c}{P_{y,c}} = \frac{1{,}220 \text{ kips}}{2{,}800 \text{ kips}}$$
$$= 0.436 > 0.2$$

$$k_{2,c} = \frac{9}{8}(1 - 0.436)$$
$$= 0.635$$

With two beam plastic hinges, two column plastic hinges, and a strain hardening factor of 1.1, the moment frame shear is:

$$V_m = \frac{1.1(2)}{h}(M_{u,b}k_{1,b}k_{2,b} + M_{u,c}k_{1,c}k_{2,c})$$
$$= \frac{1.1(2)}{132 \text{ in.}}\left[(11{,}900 \text{ kip-in.})(1.36)(0.666) + (17{,}300 \text{ kip-in.})(1.22)(0.635)\right]$$
$$= 403 \text{ kips}$$

This is 34% of the total frame shear of 1,200 kips. This distribution of the shear in this frame is within reasonable agreement with the test results of V_m = 58% [refer to Figures 6 and 9 of Lopez et al. (2002)] in view of the stiffening effects of the frame by the loading truss that was required for testing.

SUMMARY

A rationale is presented herein for buckling-restrained braced frames that includes the inherent moment frame forces when the frame is subjected to seismic forces and displacements. An evaluation of the distribution of the story shear between the braces and the moment frame is made using conventional plastic analysis of the moment frame. This rationale may be used to optimize the story shear distribution to mitigate the effects of the frame distortion forces when the frame is subjected to large seismic and wind loadings. An evaluation of the lateral force distributions in a typical frame by FEA and in the simulated Lopez test frame by the rationale presented herein showed an agreement between the FEA and the laboratory test and analytical model force distributions that supports the rationale presented herein.

REFERENCES

AISC (2022a), *Seismic Provisions for Structural Steel Buildings*, ANSI/AISC 341-22, American Institute of Steel Construction, Chicago, Ill.

AISC (2022b), *Specification for Structural Steel Buildings*, ANSI/AISC 360-22, American Institute of Steel Construction, Chicago, Ill.

AISC (2023), *Steel Construction Manual*, 16th Ed., American Institute of Steel Construction, Chicago, Ill.

ASCE (2022), *Minimum Design Loads and Associated Criteria for Buildings and Other Structures*, ASCE/SEI 7-22, American Society of Civil Engineers, Reston, Va.

ASTM (2020), *Standard Specification for Structural Steel Shapes*, A992/A992M-20, ASTM International, West Conshocken, Pa.

Lopez, W.A., Gwie, D.S., Lauck, T.W., and Saunders, C.M. (2004), "Structural Design and Experimental Verification of a Buckling-Restrained Braced Frame System," *Engineering Journal*, AISC, Vol. 41, No. 4, pp. 177–186.

Lopez, W.A., Gwie, D.S., Saunders, C.M., and Lauck, T.W. (2002), "Lessons Learned from Large-Scale Tests of Unbonded Braced Frame Subassemblies," *Proceedings of the Structural Engineers Association of California 2002 Convention*.

Mahin, S. and Patxi, U. (2002), "Summary of Full Scale Braced Frame Test Using Buckling Restrained Braces," UCB 2002 Test 3, University of California, Berkeley, Calif.

Muir, L.S. and Thornton, W.A. (2014), *Vertical Bracing Connections—Analysis and Design*, Design Guide 29, AISC, Chicago, Ill.

Richard, R.M., Radau, R.E., and Allen, J. (2017), "Damage Tolerant Braced Frame Designs," *Proceedings of the Structural Engineers Association of California 2017 Convention*.

Walters, M.T., Maxwell, B.H., and Berkowitz, R.A. (2002), "Design for Improved Performance of Buckling-Restrained Braced Frames," *Proceedings of the Structural Engineers Association of California 2002 Convention,* pp. 507–513.

APPENDIX A
DERIVATION OF COEFFICIENTS

Derivation of k_1

A braced-moment frame with hinged beams is shown in Figure A-1. Because the hinges are offset from the beam ends, the hinge rotation, θ_h, exceeds the story drift angle, θ, as shown in Figure A-2, where L is the beam length.

The hinge rotation is calculated as:

$$\begin{aligned}\theta_h &= \theta + \frac{2\theta L_h}{L - 2L_h} \\ &= \theta\left(1 + \frac{2L_h}{L - 2L_h}\right) \\ &= \theta k_1\end{aligned} \tag{A-1}$$

where

$$\begin{aligned}k_1 &= 1 + \frac{2L_h}{L - 2L_h} \\ &= \frac{L}{L - 2L_h}\end{aligned} \tag{A-2}$$

A generalized braced frame (i.e., chevron or diagonal) may have moment hinge lengths, $L_{h,a}$ and $L_{h,b}$, that differ on either side of the member. For this case, k_1 differs on each side of the member and is calculated separately for each side as:

$$\begin{aligned}k_{1,a} &= 1 + \frac{2L_{h,a}}{L - L_{h,a} - L_{h,b}} \\ &= \frac{L + L_{h,a} - L_{h,b}}{L - L_{h,a} - L_{h,b}}\end{aligned} \tag{A-3}$$

$$\begin{aligned}k_{1,b} &= 1 + \frac{2L_{h,b}}{L - L_{h,a} - L_{h,b}} \\ &= \frac{L - L_{h,a} + L_{h,b}}{L - L_{h,a} - L_{h,b}}\end{aligned} \tag{A-4}$$

The member shear is calculated by adding the working point moments, which only differ by the factors $k_{1,a}$ and $k_{1,b}$, and dividing by the member length. An effective k_1 factor can be calculated as:

$$\begin{aligned}k_1 &= \frac{k_{1,a} + k_{1,b}}{2} \\ &= \frac{L}{L - L_{h,a} - L_{h,b}}\end{aligned} \tag{A-5}$$

This formulation can be used for all frame calculations when member hinge locations relative to the working points are known. Note that for the symmetric case where $L_{h,a} = L_{h,b} = L_h$, k_1 simplifies to the general case. When only one hinge exists on a member, as with columns in the column mechanism, setting one hinge length to zero provides an accurate yet conservative result for the moment frame proportion of the base shear.

Derivation of k_2

The beam plastic moment capacity, M_p, is evaluated using beam-column interaction equations given in AISC *Specification* Section H1 (AISC, 2022b). Assuming the beams (with gross area, A_b, and strong-axis plastic modulus, Z_x) are in uniaxial bending, the moment capacity for a given axial load, P, is found by rearranging the equations:

$$k_2 = \frac{M_p}{M_u} = \begin{cases} \dfrac{9}{8}\left(1 - \dfrac{P}{P_y}\right), \text{ for } \dfrac{P}{P_y} \geq 0.2 \\ 1 - \dfrac{P}{2P_y}, \text{ for } \dfrac{P}{P_y} < 0.2 \end{cases} \tag{A-6}$$

where

$$P_y = F_y A_b \tag{A-7}$$

$$M_u = F_y Z_x \tag{A-8}$$

APPENDIX B
FINITE ELEMENT ANALYSIS RESULTS

Shown in Figure B-1 is the FEA model used to analyze the Figure 6 truss. Beams, columns, braces, and plates were modeled using 20-node hexahedrons. Fillet welds were modeled using 10-node tetrahedrons. The BRB core area yield stress was 42 ksi. This FEA model comprised approximately 468,000 nodes and 96,000 elements (Richard et al., 2017).

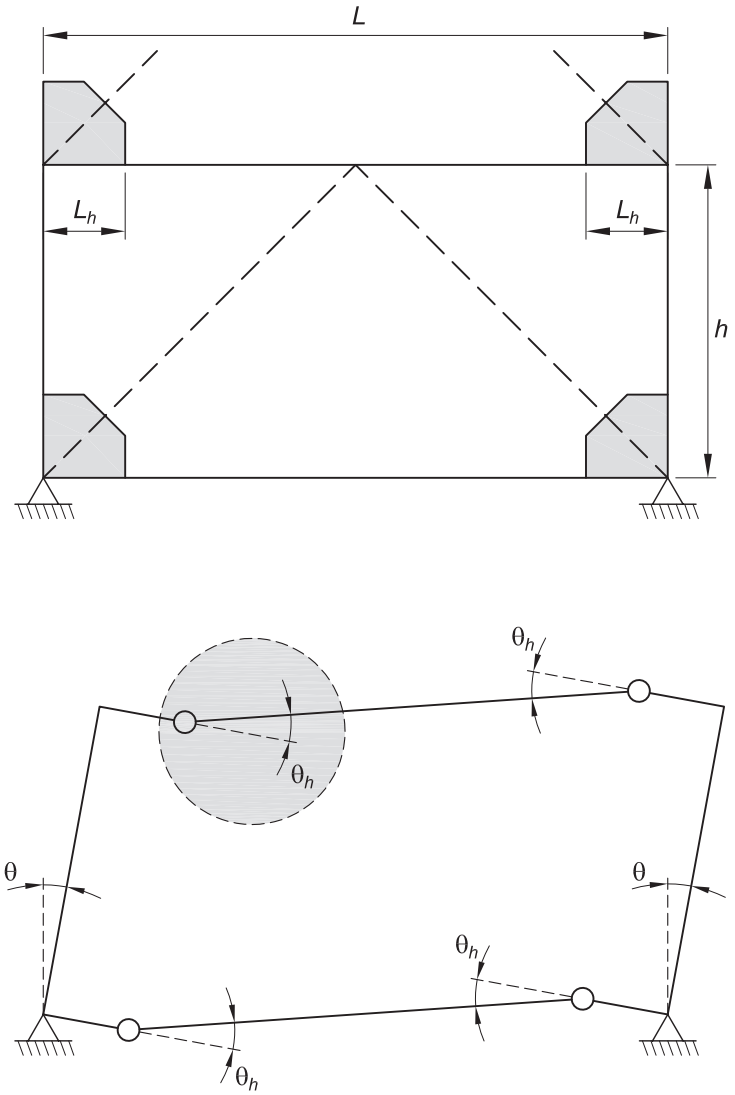

Fig. A-1. Moment frame story geometry and plastic hinge mechanism.

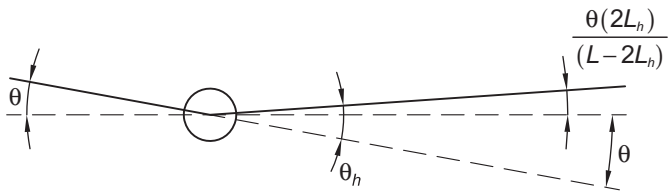

Fig. A-2. Magnified view of plastic hinge rotation from Figure A-1.

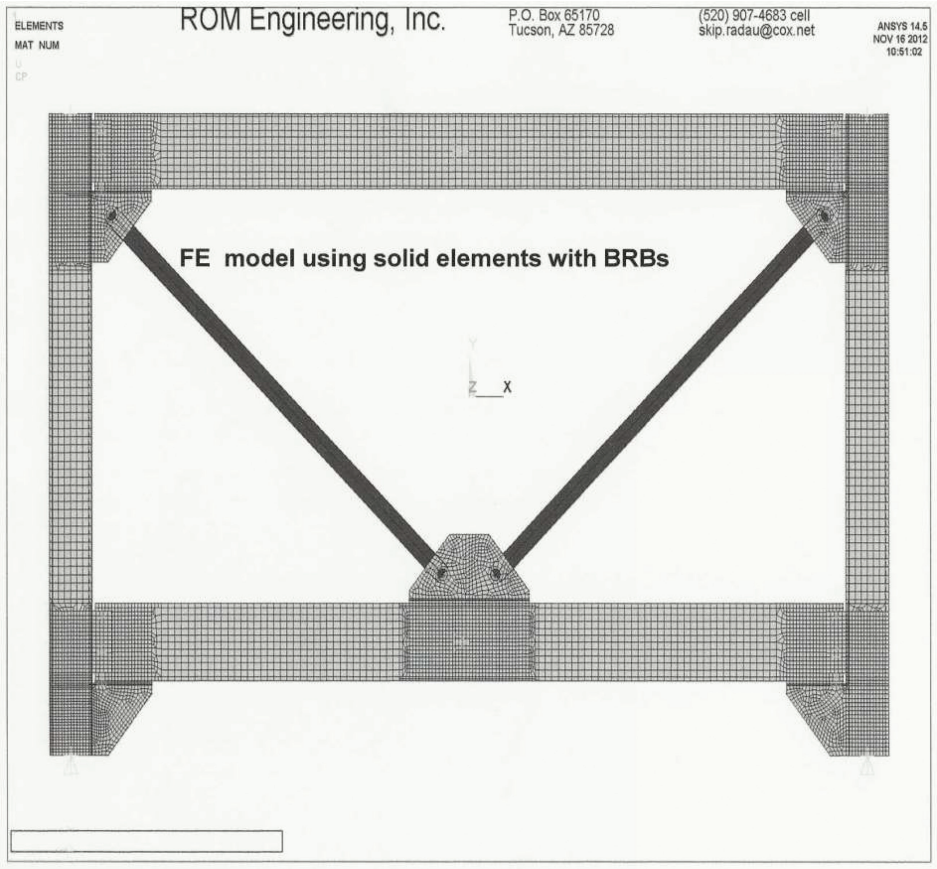

Fig. B-1. Finite element model of the frame shown in Figure 6.